JOURNAL OF APPLIED ELECTROCHEMISTRY 21 (1991) 175–180

Carbon activity measurement using a solid state potentiometric cell: application to boron carbides

K. FROMENT

Laboratoire des Matériaux Absorbants, D. Tech., C.E.N. Saclay, 91191 Gif sur Yvette, France

J. FOULETIER, M. FOULETIER*

Laboratoire d'Ionique et d'Electrochimie des Solides (L.I.E.S.-G.), E.N.S.E.E.G.-I.N.P. Grenoble, BP 75, 38402 Saint Martin d'Hères Cedex, France

Received 19 January 1990; revised 24 April 1990

The interface between β-alumina and carbonaceous materials has been studied from both thermodynamic and electrochemical viewpoints. Based on the results, a solid electrolyte potentiometric cell has been devised and the conditions enabling carbon activity to be measured have been determined. In spite of the chemical inertness of the materials involved, the measurements must be performed at low temperature ($T < 720\,\mathrm{K}$). Carbon activity measurements in the boron-carbon system are presented.

1. Introduction

Boron carbides are used as neutron absorbents in nuclear engineering. At present, the most widely used carbide has a chemical composition near B_4C. The materials are manufactured in the form of sintered pellets and stacked in steel containers. One of the main problems encountered during their service life is their chemical reaction with the metallic containers. One way of preventing steel carburization would be to substitute a compound with a carbon activity smaller than that of the steel containers, which is in the range 10^{-2} to 10^{-1} [1], for the two-phase (B_4C + C) material.

The widely accepted phase diagram of the B–C system was first proposed by Elliott [10]. A single phase domain (referred to as β) ranges from 9 mol % ($B_{10}C$) to 20 mol % (B_4C) (see Fig. 1). At 20 mol % C, the B_4C compound is in equilibrium with a carbon rich solid solution (about 99 mol % C) and the $B_{10}C$ compound is in equilibrium with a boron-rich solid solution (99.8 to 99.9 mol % B). The solubilities of C and B in the two solid solutions are so low that B_4C and $B_{10}C$ can be considered in equilibrium with pure C and B, respectively. Accordingly, the carbon activity in B_4C and the boron activity in $B_{10}C$ can be assumed to be unity.

The Gibbs energy of formation of B_4C is known with accuracy but the data corresponding to other compositions have yet to be determined. In order to measure the activity of carbon in the compounds of the boron-carbon system, various methods can be considered, involving solid-gas or all solid state equilibria.

Direct measurements of carbon activity have been carried out by solid-gas equilibrium methods on U-C and Fe-C alloys [2, 3]. We found it was impossible to use this method in boron carbide compounds at 1170 K because of the too slow diffusion processes [4]. In the temperature range 1770–2470 K one of the authors [4] has measured the carbon activity in boron carbides using Knudsen effusion cells and a mass spectrometer.

Potentiometric cells using CaF_2 as a solid electrolyte have been used for thermodynamic investigations of thorium, uranium, manganese and chromium carbides [5–7]. The direct measurement of carbon activity in Fe-C alloys has been carried out in the 873–1073 K range using a FeC, $CaC_2/CaF_2/CaC_2$, C cell. However, due to the water sensitivity of calcium carbide, a very careful treatment was required [8]. In the present work, we use β-alumina as a solid electrolyte and Al_4C_3, which is less reactive than CaC_2, as a carbide at each electrode, as has been proposed by Obata *et al.* [9]

The aim of this paper is to present the measurement of carbon activity in boron carbides at temperatures lower than 720 K, using solid state potentiometric cells involving sodium β-alumina as the solid electrolyte.

2. Experimental details

2.1. *Boron carbide synthesis*

The boron carbide powder, obtained by reduction of B_2O_3 by magnesium with the addition of carbon, was purchased with a B_4C composition from Quartz and Silice (Du Pont de Nemours). The powder was heated to 2070 K to eliminate volatile impurities. The B_4C

---

* Presently at Electrochimie Moléculaire, CENG, DRF. LCH/EM, 85X, 38041 Grenoble Cedex, France.

0021-891X/91 $03.00 + .12

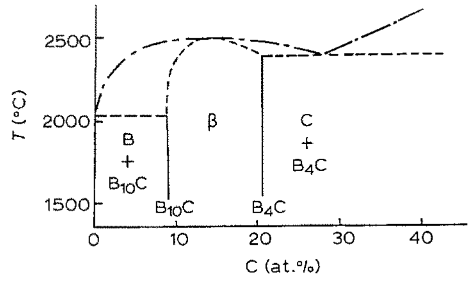

Fig. 1. Phase diagram of the boron-carbon system, from Elliott [10].

powder was then mixed with boron to obtain the desired composition. The mixture was heated to 2170 K in a graphite crucible coated with boron nitride to avoid direct contact with graphite. The sintered pellet was ground and the boron and carbon compositions were determined by chemical analysis [4].

2.2. *Chemicals*

Graphite powder (t5N5) and aluminium carbide were purchased from Alpha. Argon U was supplied by Air Liquide.

2.3. *Experimental set-up*

A previously described [11] two-compartment cell was used (Fig. 2). The β-alumina (Alcoa) pellet (1) (3 mm thick, 25 mm diameter) was machined from a block, sintered at 1650° C for 2 h after isostatic pressing under 2 tons cm^{-2}. The pellet was held between two α-alumina tubes with gold O-rings inserted between the tubes and the pellet to ensure gas tightness. The lower tube (2) was fixed to the external coaxial alumina tube (3) in its cold part with a resin (Torr seal, Varian). The upper tube (4) slid inside the outer tube (3) which enabled us to maintain pressure on the gold rings by means of stainless steel springs. Gas tightness was found to be very good up to 1000° C [12]. The cell was then put into a resistance furnace. The lower face of the β-alumina pellet, coated with a platinum paint (Degussa 308 A) and in contact with air at 1 atm pressure, was used as the air-reference electrode using a platinum wire (5) as the current lead.

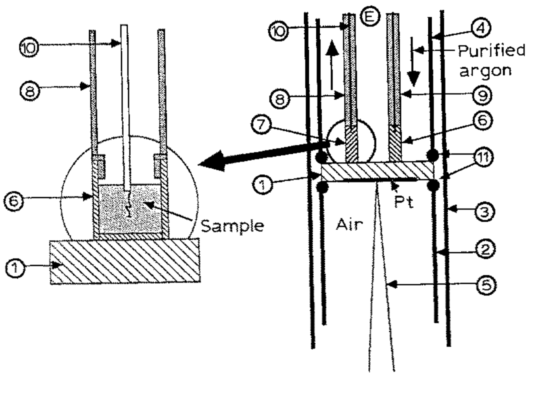

Fig. 2. Two-compartment cell. (1) β-alumina pellet; (2), (3), (4) α-alumina tubes; (5) Pt-Pt 10% Rh thermocouple; (6), (7) β-alumina crucibles; (8), (9) α-alumina capillaries; (10) platinum wire; (11) gold O-rings.

In order to maintain a very low oxygen pressure in the upper part of the cell, the gas circuit used consisted of gas tanks (Ar, CO_2 or Ar-H_2), an oxygen electrochemical pump and an oxygen zirconia sensor. We have demonstrated that with such equipment, the oxygen pressure can be accurately monitored over the range $1\text{–}10^{-27}$ atm [13].

Two crucibles machined from a β-alumina block of the same composition as the pellet (4 mm in diameter, 10 mm long) were put in contact with the upper face of the pellet (1). Each crucible was filled with the finely ground carbide mixtures. The crucibles were maintained in contact with the pellet using alumina capillaries (8) and (9). A platinum/platinum (10 %) rhodium thermocouple (10) was used for the sample temperature and the carbon activity measurements.

3. Thermodynamic considerations

3.1. *Constituents and phases*

Potentiometric measurements can be carried out only on systems with a degree of freedom of unity. Then, at a given temperature, the activities of all the components are fixed. For example, let us consider cell (I):

$$\text{Pt, } B_4C(\text{argon}) \,|\, \beta\text{-alumina} \,|\, B_xC(\text{argon}), \text{ Pt} \qquad 4 \leqslant x \leqslant 10. \tag{I}$$

At the β-alumina/B_xC interface, five independent constituents have to be considered (carbon, aluminium, oxygen, sodium and boron) and four phases are present, namely, a gaseous phase and three solid phases, i.e. β-alumina, α-alumina and boron carbide. Under these conditions, the degree of freedom of the system is 3. Thus, at given temperature and pressure (which is nominally fixed at 1 atm), the system is not completely defined. It is necessary to fix the chemical potential of one of the components. Choudhury [14] obtained stable and reproducible e.m.f. measurements with electrodes fixing either the oxygen chemical potential (using metal-metal oxide mixtures at both electrodes) or the aluminium chemical potential (using cells such as Al | β-alumina | AlF_3, NiF_2, Ni or Al | β-alumina | NaF, NiF_2, Ni).

3.2. *Oxygen potential in the cell*

In the experimental set-up, the presence of minute quantities of oxygen cannot be avoided. The oxygen mole fraction was evaluated to be $\sim 10^{-6}$. Oxygen is able to combine with carbon according to the reactions:

$$C + \tfrac{1}{2}O_2 = CO \qquad [1]$$

$$C + O_2 = CO_2 \qquad [2]$$

The corresponding equilibrium constants are:

$$K_1 = p(CO)/p(O_2)^{1/2}a_C \qquad (1)$$

$$K_2 = p(CO_2)/p(O_2)a_C \qquad (2)$$

The argon flow rate, being very small and the electrode materials being in large excess, it can reasonably be assumed that the equilibrium between carbon and oxygen is reached at the operating temperature. It is therefore possible to compute the partial pressure of all the gaseous constituents as functions of the initial oxygen content and in the presence of various carbon activities.

Taking

$$\lambda = 2p(O_2) + p(CO) + 2p(CO_2) \qquad (3)$$

the following equations can be derived

$$p(O_2)^{1/2} = \{[K_1^2 a_C^2 + 8\lambda(K_2 a_C + 1)]^{1/2} - K_1 a_C\}/4(K_2 a_C + 1) \qquad (4)$$

$$p(CO) = K_1 a_C\{[K_1^2 a_C^2 + 8\lambda(K_2 a_C + 1)]^{1/2} - K_1 a_C\}/4(K_2 a_C + 1) \qquad (5)$$

$$p(CO_2) = (K_2 a_C)^{1/2}\{[K_1^2 a_C^2 + 8\lambda(K_2 a_C + 1)]^{1/2} - K_1 a_C\}/4(K_2 a_C + 1) \qquad (6)$$

The oxygen partial pressure can be written as a function of the ratio:

$$p(O_2)^{1/2} = K_1 p(CO_2)/K_2 p(CO) \qquad (7)$$

which has simplified expressions in the following limiting cases:

when the major species is CO_2, then

$$p(O_2) \simeq \tfrac{1}{2} K_2 a_C \qquad (8)$$

and when the major species is CO, then

$$p(O_2)^{1/2} \simeq 1/K_1 a_C \qquad (9)$$

The variations of log $p(O_2)$ as a function of the reciprocal of the temperature are plotted in Fig. 3 for various oxygen mole fractions and for unit carbon activity.

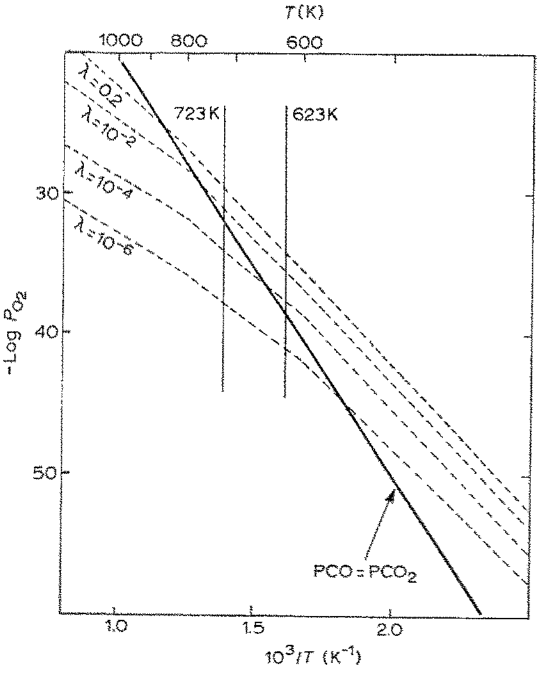

Fig. 3. Log (pO_2) with the reciprocal of temperature in the presence of carbon, for various oxygen mole fraction λ: 10^{-6}, 10^{-4}, 10^{-2}, 0.2.

From this diagram, it can be concluded that, in the temperature range investigated, oxygen is mostly converted into carbon monoxide: the oxygen partial pressure is always smaller than 10^{-30} atm and therefore $p(CO) \simeq \lambda$. Note that the carbon monoxide partial pressure is independent of the carbon activity value and is therefore the same throughout the inner compartment of the cell. On the other hand, the oxygen partial pressure is determined by the carbon activity in the material to be studied.

3.3. *The role of Al_4C_3*

The above analysis demonstrates that it is necessary to fix the aluminium chemical potential. According to Obata *et al.* [9], this can be done by mixing Al_4C_3 powder with both electrodes: the degree of freedom is lowered to 1 as the number of phases is increased while the number of constituents remains constant.

This point was verified experimentally. Note that the e.m.f. of the cell:

$$\text{Pt, } C_{\text{graphite}}, Al_4C_3(\text{argon}) \,|\, \beta\text{-alumina} \,|\, C_{\text{graphite}}, Al_4C_3(\text{argon}), \text{Pt} \qquad [II]$$

is equal to zero whatever the temperature (straight line (d) in Fig. 4). On the contrary, this is not the case for the cell:

$$\text{Pt, } B_4C, Al_4C_3(\text{argon}) \,|\, \beta\text{-alumina} \,|\, C_{\text{graphite}}, Al_4C_3(\text{argon}), \text{Pt} \qquad [III]$$

(Fig. 4 line (e)): in the latter electrochemical chain, the chemical potential of boron was not fixed. As shown in Fig. 4 (lines (a), (b) and (c)), e.m.f. results carried out on cells of type [I] give erroneous results corresponding to positive values of the partial free enthalpy of carbon. This demonstrates the necessity of adding Al_4C_3 to the electrode materials in order to get reproducible results: this compound does not form spontaneously at the interface between carbonaceous materials and β-alumina.

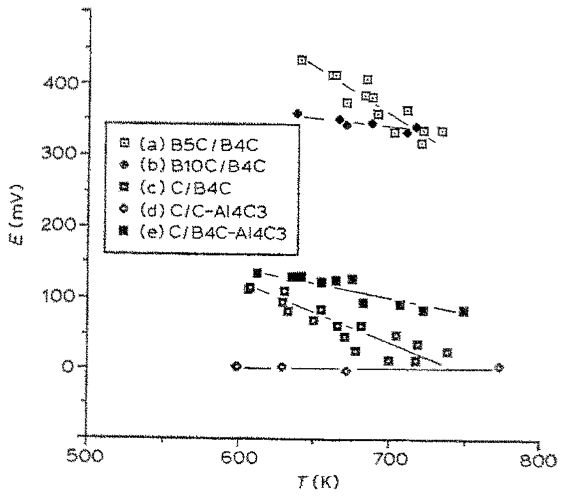

Fig. 4. E.m.f. against temperature for various cells with carbon or carbides as electrode materials.

Moreover, Al_4C_3 is an ionically conducting material; its conductivity is of the order of $10^{-6}\,\Omega^{-1}\,cm^{-1}$ at 650 K [9]. Thus, the addition of Al_4C_3 to boron carbides has the additional advantage of decreasing the resistivity of the electrode material. This property becomes very important as the boron content increases and the temperature is lowered. Thus, the carbon activity measurements were performed using such cells as:

$$\text{Pt, } B_4C + Al_4C_3(\text{argon}) \,|\, \beta\text{-alumina} \,|\, B_xC + Al_4C_3(\text{argon}), \text{ Pt} \qquad [IV]$$

In every case, an initial period of 2 to 15 days was necessary to obtain a stable e.m.f. to within less than 1 mV. After a change of the cell temperature, a stable e.m.f. was obtained after 1 to 7 days.

3.4. *Electrode reaction study*

The use of β-alumina in solid electrolyte oxygen sensors has been suggested by various authors [14, 15] but, to our knowledge, the oxygen electrode reaction has never been investigated in detail. In fact, the cells have been used only at very low oxygen pressures, corresponding to metal-metal oxide equilibria.

In our experimental set-up (Fig. 2), the platinized outer surface of the β-alumina pellet, in contact with air, was used as the reference electrode of the cell. A platinum point electrode was put in contact with the upper surface of the pellet in the inner cell compartment. This cell was tested in the range 10^{-1}–10^{5} Pa at temperatures between 400 and 900 K.

At low oxygen pressure, corresponding to an oxygen mole fraction in argon lower than 10^{-3} or to metal–metal oxide systems such as Cu–Cu_2O, a rather short response time was observed, even at temperatures lower than 500 K. At high oxygen pressure, large response times and scattered e.m.f. measurements were obtained. This behaviour is very different from what is observed with classical zirconia based oxygen sensors but can be satisfactorily explained by the electrode reaction scheme proposed by GROS *et al.* [16] for β-alumina.

Any electrode reaction occurring at the β-alumina surface may involve both sodium and oxygen ions. Generally, sodium, which is the most mobile ion in the β-alumina structure, is considered to be the only exchanged species at the interface. This is particularly true at low oxygen pressure, for which sodium is the major component in the gas phase. For example, at 1000 K, with an oxygen pressure around 10^{-15} Pa, the sodium pressure in equilibrium with β-alumina ranges between 10^{-2} to 10^{-4} Pa. In these conditions, sodium ions can exchange rapidly at the electrode interface. However, under high oxygen pressure, sodium becomes a minor component and the sodium exchange becomes very slow. At relatively high temperatures, owing to the small anionic conductivity of β-alumina [17, 18] an additional oxygen flux through the interface is possible. This results in a non-stationary state corresponding to the observed continuous drift of the electrode potential [16].

From the above thermodynamic calculations, it was concluded that under the experimental conditions prevailing in the cell, the oxygen partial pressure was always smaller than 10^{-30} atm. The sodium partial pressure in the gas phase above the electrolyte is therefore always much larger than the oxygen partial pressure. These conditions are convenient for a reversible sodium exchange electrode reaction, enabling significant measurements to be performed.

3.5. *Possible electrode reaction mechanism*

All the results presented here are consistent with an electrode reaction mechanism involving sodium exchange between the electrolyte and the surrounding medium, such as, for instance:

$$Al_4C_3 + 6Na_2O\,(\beta\text{-alumina}) = 2Al_2O_3 + 12Na^+ + 12e^- + 3C \qquad [3]$$

In Fig. 5 the variation of log (P_{CO}), corresponding to the formation of Na_2CO_3 from Na_2O, $NaAlO_2$ and $NaAl_{11}O_{17}$, are plotted as a function of the reciprocal temperature together with log (P_{CO}) variations for various oxygen mole fractions. Under the experimental conditions prevailing in this study, the carbon monoxide mole fraction was $\sim 10^{-5}$: it can be seen from Fig. 5 that CO cannot disproportionate into carbon and sodium carbonate from reaction with β-alumina. Then, the activity of sodium oxide in β-alumina is a constant and the electrode potential corresponding to Reaction [3] is solely determined by the value of carbon activity in the electrode material.

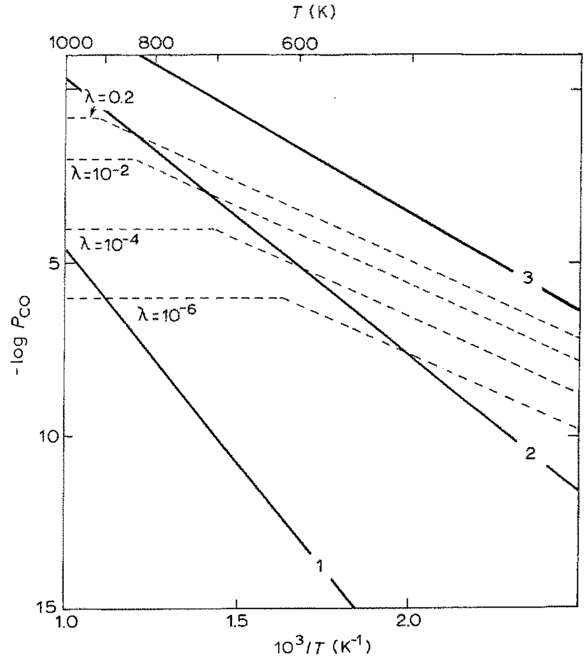

Fig. 5. Equilibrium carbon monoxide pressure versus the reciprocal of temperature for (1) reaction $Na_2CO_3 + C = Na_2O + 2CO$, (2) reaction $Na_2CO_3 + C + Al_2O_3 = NaAl_2O + 2CO$, (3) reaction $Na_2CO_3 + C + 11Al_2O_3 = 2NaAl_{11}O_{17} + 2CO$. (– – –) Oxygen mole fraction $\lambda = 10^{-6}, 10^{-4}, 10^{-2}, 0.2$.

The carbon monoxide does not take part in the electrode reaction balance. However, it can play a kinetic role, as an intermediate in the exchange between elemental carbon and its fully oxidized form. In this respect, the initial period before obtaining stable measurements can be interpreted as the time needed to reach the carbon-oxygen equilibrium in the gas phase.

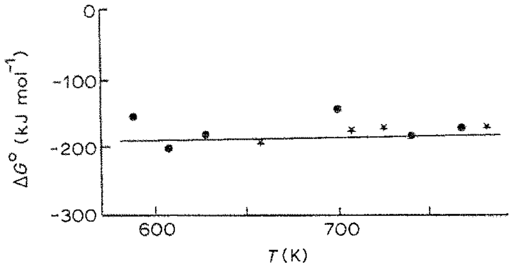

Fig. 6. Gibbs free energy of formation of Al_4C_3 against temperature (——) from JANAF [19] (∗∗∗) after OBATA *et al.* [9]; (●●●) our results.

4. E.m.f. measurements

4.1. *Cell e.m.f.*

The e.m.f. of this cell can be easily calculated assuming:

- equilibrium established at both electrodes,
- both electrode materials surrounded by the same atmosphere,
- the β-alumina electrolyte is a pure sodium ion conductor,
- the activity of Na_2O in β-alumina is the same at both electrodes

The e.m.f., E_{IV}, of the cell (IV) obeys the Nernst equation:

$$E_{IV} = (RT/4F)\ln[(a_C)_y/(a_C)_z] \qquad (10)$$

where the subscripts y and z refer to the two crucibles set on the upper face of the β-alumina pellet.

The B_4C composition is actually a $(B_4C + C)$ mixture close to the phase boundary, corresponding to a unit carbon activity in the reference electrode of the cell. Under these conditions, the carbon activity in the B_xC samples, $a_C[B_xC]$, can be deduced from the e.m.f., E_{IV}, of the cell by using the equation:

$$E_{IV} = (RT/4F)\ln a_C[B_xC]. \qquad (11)$$

4.2. *Evaluation of $\Delta G_f^0(Al_4C_3)$.*

To check the correct operation of the set-up, the standard Gibbs energy of formation of Al_4C_3, $\Delta G_f^0(Al_4C_3)$, was measured using the cell:

$$\text{Pt, Al} + Al_4C_3(\text{argon})\,|\,\beta\text{-alumina}\,|\,Al_4C_3 + C_{\text{graphite}}(\text{argon}),\ \text{Pt} \qquad [V]$$

The e.m.f. of the cell, E_V, is proportional to ΔG_f^0, according to:

$$E_V = \Delta G_f^0/12F \qquad (12)$$

The measured variation of $\Delta G_f^0(Al_4C_3)$ as a function of temperature is given in Fig. 6. The results obtained agree well with measurements carried out by Obata [9] and with the data of the Janaf tables [19].

The plots of the variations with temperature of the electrode potentials of the $(Al + Al_4C_3)$ and $(C_{graphite} + Al_4C_3)$ mixtures with respect to the air reference electrode are given in Fig. 7. A change of the slope of the straight lines was observed for both systems at around 720 K. At higher temperatures, the scattering of the results was much larger. Irregularities of the e.m.f. at high temperatures has been attributed to reaction between β-alumina and electrode materials [9]. We suggest that this phenomenon can be attributed to the occurence of an electrode reaction mechanism involving the onset of a side oxygen exchange as described above.

From these preliminary experiments, it was concluded that the measurements should be conducted at temperatures as low as possible. The lower limit ($T < 350$ K) was imposed by a large increase of the impedance of the system.

4.3. *Determination of carbon activity in boron carbides*

Figure 8 shows the e.m.f. variation with temperature for various boron carbides, B_xC, with x from $x = 4$ to $x = 8$. The reference system was a $(B_4C + C)$ mixture. Straight lines were obtained with rather good correlation coefficients ranging between 0.95 and 0.99. The carbon activity can be deduced directly from Equation 2. Small variations of carbon activity with temperature were observed. The variation of carbon activity with composition at 670 K is given in Fig. 9. In the β-domain, a monotonic decrease of carbon activity was observed as the boron content increased. The carbon activity can be extrapolated to 7×10^{-6}. On the other hand, the boron activity in B_xC can be estimated from the Gibbs energy of formation of B_4C [19]:

$$\Delta G_f^0(B_4C) = 4RT\ln a_B + RT\ln a_C \qquad (13)$$

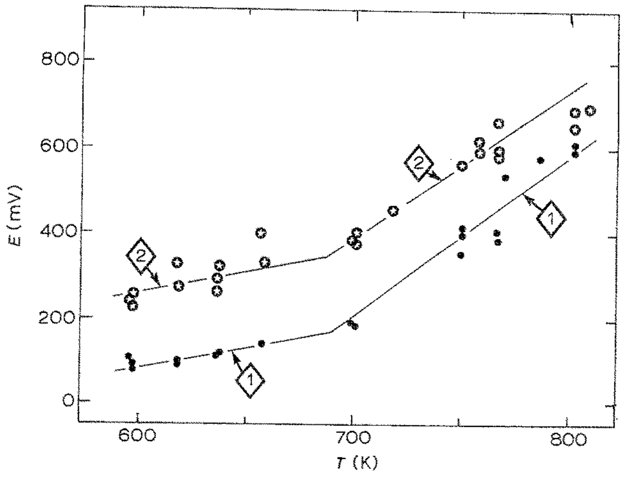

Fig. 7. E.m.f. against temperature of the $(Al + Al_4C_3)$ mixture (curve 2) and $(C_{graphite} + Al_4C_3)$ mixture (curve 1) using an air reference electrode.

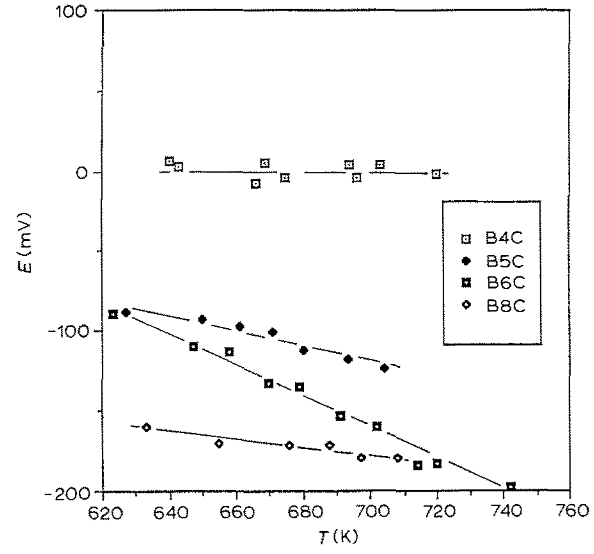

Fig. 8. E.m.f. and partial Gibbs free enthalpy of carbon against temperature for various boron carbides, B_xC ($4 \leqslant x \leqslant 8$).

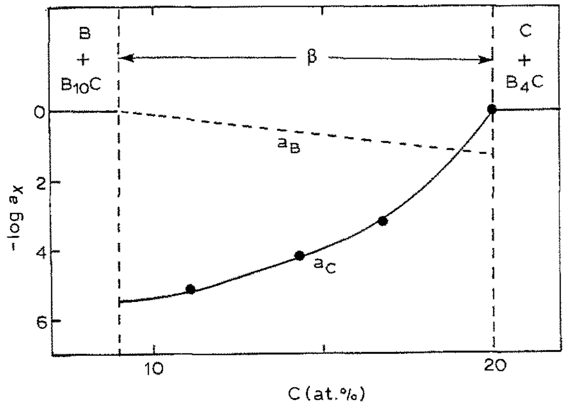

Fig. 9. Carbon and boron activity variations with composition at 673 K.

At 670 K, small variations of the boron activity in the β-domain were observed i.e. from 1 ($x = 10$) to 6×10^{-2} ($x = 4$) (see Fig. 9).

The chemical stability of the $B_xC + Al_4C_3$ mixture sets another limit. Due to the excessively low carbon activity compared to that of Al_4C_3, it was not possible to obtain stable e.m.f. with samples richer in boron than B_8C.

5. Conclusion

In this study, it was demonstrated that carbon activity measurements in boron carbides can be carried out at low temperatures using β-alumina as the solid electrolyte, provided the following experimental conditions are fulfilled:

(i) the oxygen pressure around the samples is very low so that oxygen is quantitatively converted to carbon monoxide in the presence of carbon.

(ii) the temperature is kept lower than 720 K in order to avoid side reactions due to oxygen mobility in β-alumina. Considering the large impedance of the cell at low temperature, the available temperature range is rather narrow, i.e. $600\,K < T < 720\,K$.

(iii) the aluminium activity is fixed at both electrodes by adding Al_4C_3 to the electrode materials,

(iv) the reference electrode must be a (B_4C + C) two-phase mixture.

The carbon activity in the single-phase domain ranges from 1 to about 10^{-6}. The increase of boron content in boron carbide corresponds to a noticeable reduction of the carbon activity and therefore of the carburizing activity of the metallic containers; simultaneously a small variation of the boron activity was observed.

References

[1] J. Rouault, Thesis E.C.A., Paris, 1979.
[2] P. P. Smith, *J. Am. Chem. Soc.* **68** (1963) 1163.
[3] M. Tetenbaum and P. D. Hunt, *J. Nucl. Mat.* **40** (1971) 104.
[4] K. Froment, Thesis, Univ., Paris, **6** (1989).
[5] W. K. Behl and J. J. Egan, *J. Electrochem. Soc.* **113** (1966) 376.
[6] T. Satow, *J. Nucl. Mat.* **21** (1967) 249, 255.
[7] F. Moattar and J. J. Anderson, *Trans. Faraday Soc.* **67** (1971) 2303.
[8] T. Kirihara, N. Obata and T. Saida, 75th Annual Meeting of Japan Institute of Metals (1974) Paper J. II 198.
[9] N. Obata, H. Sakai, M. Tachiki, M. Yamada and T. Kirihara, *Solid State Ionics* **3/4** (1981) 551.
[10] R. P. Elliott, 'Constitution of Binary Alloys,' 1st Suppl., McGraw-Hill, New York (1965) p. 110.
[11] J. Fouletier and M. Hénault, *Solid State Ionics* **9/10** (1983) 1277.
[12] J. Amossé, J. Fouletier and M. Kleitz, *Bull. Mineral.* **105** (1982) 188.
[13] A. Caneiro, E. Siebert and J. Fouletier, 'Adv. in Ceramics,' Vol. 12, 'Science and Technology of Zirconia II,' The Am. Ceram. Soc. (1984) p. 618.
[14] N. S. Choudhury, *J. Electrochem. Soc.* **120** (1973) 1663.
[15] F. A. Elrefaie and W. W. Smeltzer, *ibid.* **128** (1981) 1443.
[16] P. Gros, C. Chatillon and M. Fouletier, to be published.
[17] L. C. De Jonghe and A. Buechele, *J. Mat. Sci.* **17** (1982) 885.
[18] R. O. Ansell, A. Gilmour and R. J. Cole, *J. Electroanal. Chem.* **244** (1988) 123.
[19] Janaf Thermochemical Tables, 'Handbook of Chemistry and Physics,' NBS 37, Washington DC, **14**, Suppl. 1 (1985).